



A novel approach of preparing TiO₂ films at low temperature and its application in photocatalytic degradation of methyl orange

Yanrong Zhang*, Jing Wan, Youqing Ke

Environmental Science Research Institute, Huazhong University of Science and Technology, 1037 Luoyu Road, Wuhan 430074, PR China

ARTICLE INFO

Article history:

Received 26 August 2009

Received in revised form

21 December 2009

Accepted 22 December 2009

Available online 4 January 2010

Keywords:

Non-calcinated TiO₂ film

Electrophoretic deposition

Photocatalytic activity

Methyl orange degradation

ABSTRACT

Here we introduce a novel approach of preparing TiO₂ films on conductive substrates at low temperature by electrophoretic deposition method without successive calcinate treatment. The photocatalytic activity of the non-calcinated TiO₂ film was evaluated by degradation rate of methyl orange (MO). We found that the degradation rate of MO increased with the amount of TiO₂, and it was higher in both acidic and alkaline media than under neutral condition. In addition, lower pH was more favorable for the degradation of MO. The photocatalytic degradation of MO could be described as pseudo-first order reactions. When the initial concentration of MO increased from 1 mg/L to 10 mg/L, the highest degradation rate was achieved at 5 mg/L. The apparent reaction rate constant was calculated to be 0.0098 min⁻¹.

© 2009 Elsevier B.V. All rights reserved.

1. Introduction

In 1972, the publication about photocatalytic degradation of water on the titanium oxide (TiO₂) electrode by Japanese scholars Fujishima and Honda [1] raised the curtain on the study of photocatalysis. In 1976, Carey et al. [2] found that after irradiated by UV light, TiO₂ was capable to catalyze the dechloridization of polychlorobiphenyl (a group of organic pollutants) in water, which initiated the application of the photocatalytic technology on environmental remediation. In the past decades, TiO₂ has been applied in decomposition and mineralization of some persistent organic pollutants (POPs) such as phenols, chlorophenols, pesticides, herbicides, benzenes, humic acids and others [3–7], as well as water and air purification [8–12].

However, for the particulate TiO₂ suspension, removal of the catalyst after use is expensive and technologically difficult. Recently, the use of TiO₂ thin films for the purpose of solving environmental issue has emerged. Compared to powder TiO₂ particles, immobilized TiO₂ films are more promising in practical applications, especially in water treatment [13,14].

Conventional methods to prepare TiO₂ thin films can be classified into three categories: gas-phase preparation [15], liquid-phase preparation [15] and electrochemical preparation [15–17]. The first two methods require expensive equipments, high temperature treatment, as well as complicated procedures, and are consequently

energy-consuming. The electrochemical preparation method is relatively simple, the size and shape of TiO₂ nano-particles can be well controlled [15,16]. Therefore, it has been widely used in recent years.

Different methods have been investigated to produce semi-conducting TiO₂ films with different functions. Electrochemical anodization of metal Ti followed by calcination can be used to fabricate TiO₂ nanowires, nanorods and nanotubes [18–20]. The preparation of TiO₂ films with photocatalytic function is conventionally accomplished through electrophoretic deposition followed by calcination at high temperature [21,22]. By using the TiO₂ film prepared on the stainless steel substrate, successful photo-degradation of formaldehyde gas [23] had been demonstrated.

Here, our laboratory developed a novel method to prepare TiO₂ films with photocatalytic function at low temperature by an electrochemical method. We prepared TiO₂ films on different conductive substrates such as nickel network, aluminium plates and conductive glass plates. The experiments were conducted at low temperature, and the calcination step is not required. The photocatalytic treatment of wastewater by our TiO₂ films was demonstrated with a model pollutant methyl orange (MO).

2. Experimental

2.1. Chemicals and instruments

High-purity (99.99%) nickel network and aluminum plates were purchased from Beijing Non-ferrous Metal Co., Ltd., China. Tetra-butyl titanate (Tianjin Fuchen Chemical Reagent Co., Ltd.), isopropyl

* Corresponding author. Tel.: +86 27 87793001; fax: +86 27 87793001.

E-mail address: yanrong.zhang@yahoo.cn (Y. Zhang).

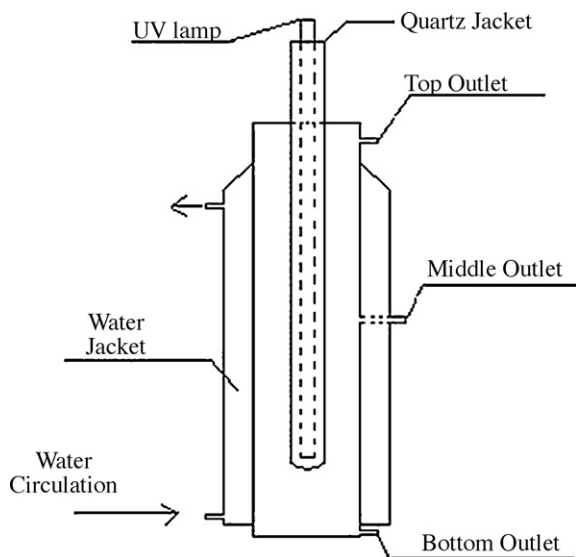


Fig. 1. Schematic diagram of the photocatalysis reactor.

alcohol (Shanghai Experimental Reagent Co., Ltd.), methyl orange (Tianjin Kemiou Chemical Reagent Co., Ltd.) and all other reagents were of analytical grade and used without further purification. Deionized water (18.0 M Ω cm) was made from Barnstead system (Barnstead).

The pH buffer solutions used in the experiments were the mixture of Na₂HPO₄ (0.2 M) and NaH₂PO₄ (0.2 M), adjusted by H₃PO₄ or NaOH to obtain the desired pH.

Cary-50 ultraviolet spectrophotometer (Varian), field emission scanning electron microscope (FESEM, SIRION 200, FEI, Netherlands) were used in the experiments. X-ray diffraction (XRD) patterns obtained on a X-ray diffractometer (PANalytical B.V.) using Cu K α radiation at a scan rate (2 θ) of 0.05° s⁻¹. The zeta potential of catalysts was determined by Zetasizer (Malvern ZS90).

2.2. Preparation of the non-calcinated TiO₂

The non-calcinated TiO₂ films were prepared as follows. The plating solution contained 17% (wt%) tetrabutyl titanate, 3% isopropyl alcohol, 3% concentrated nitric acid and 77% deionized water. The solution was first cultured for 12 h at room temperature, and then diluted 10 times before use. A constant potential (30 V) was applied between the nickel network (or aluminium plate) and a Pt electrode for 20 min. Both electrodes were immersed in the plating solution with ice/water bath.

2.3. Photocatalytic degradation of MO

The photocatalytic activity of the non-calcinated TiO₂ films was evaluated by measuring degradation rate of MO, a compound used here as a model pollutant. The experiments were carried out in a 1000 mL cylindrical glass reactor filled with 950 mL MO aqueous solution. The reactor was equipped with an ultraviolet (UV) lamp (power – 28 W with wavelength of 254 nm). The temperature of reactor was controlled by circulation of tap water inside the water jacket during degradation experiments (Fig. 1). The nickel network pieces coated with TiO₂ (8 cm × 4 cm/piece) were put into the reactor. The nickel network was first pre-saturated in the MO aqueous solution at dark for 30 min in order to reach adsorption/desorption equilibrium, then the UV lamp and water circulation were turned on to initiate degradation process. Every degradation experiment lasted 2 h, and a small sample was taken out every 15 min from the middle outlet (see Fig. 1). UV spectrometer was used to determine

the absorbance (A) of the samples ($\lambda_{\max} = 460$ nm to $\lambda_{\max} = 465$ nm with pH 2–10). Every experiment was repeated at least three times, and the average (with RSD less than 5% for three repeated results) was used as the final results. The concentration of MO was calculated from an absorbance vs. concentration calibration curve. The degradation rate (%) was evaluated by the following equation:

$$D = \frac{C_0 - C_t}{C_0} \times 100\% \quad (1)$$

where D is degradation rate, C_0 and C_t are the concentrations of the MO solution at UV irradiation time 0 and t , respectively.

3. Results and discussion

3.1. Morphology of the non-calcinated TiO₂ film

Fig. 2 illustrates the different morphologies of the nickel network before (Fig. 2(a)) and after (Fig. 2(b–d)) electroplating, respectively. It is obvious that the TiO₂ particles were successfully deposited on the nickel network (Fig. 2(b and c)). The magnified image in Fig. 2(c) showed the heterogeneity of the deposited TiO₂ on the substrate Ni network. The left and top parts of the deposited TiO₂ film in Fig. 2(c) were composed of nano-particles, while the center part had more dense structure with nanometer scale holes. Additionally, a long crack was also observed. The heterogeneous morphology of the deposited TiO₂ film might be attributed to the uneven substrate Ni network, which showed islands, alleys and cracks from the SEM image (Fig. 2(a)). The image with a higher magnification (Fig. 2(d)) shows the size of particles ranged from 30 nm to 40 nm. Heated at 450 °C for 1 h did not significantly affect the morphology of coated TiO₂ particles from SEM image (not shown here).

Fig. 3 shows XRD patterns of the as-prepared film (Fig. 3(a)) and the film (Fig. 3(b)) calcinated at 450 °C for 1 h. Both films are mainly in well-crystallized anatase phase (peaked at ca. 25.2 nm (1 0 1) and 37.6 nm (0 0 4)), but small rutile peaks were also observed at ca. 27.3 nm and 36.0 nm. Both anatase and rutile peak intensities increased slightly after calcination, which had been reported before [24,25].

The average crystallite size of anatase in the samples can be calculated with the Scherrer formula using the anatase (1 0 1) diffraction peaks:

$$D = \frac{K\lambda}{\beta \cos \theta} \quad (2)$$

where D is the average crystallite size, K is a constant (0.89 here), λ is the wavelength of the X-ray radiation (0.154 nm), β is the band broadening (full width at half-maximum) and θ is the diffraction angle. The particle sizes are calculated to be 31.3 nm and 47.0 nm for the non-calcinated and calcinated samples, respectively, which agrees well with SEM results. The particles in the calcinated samples are slightly larger than those in the non-calcinated ones, which is similar to the previous observation [23].

The TiO₂ films coated on aluminium and conductive glass plates were demonstrated to be in anatase phase as well (data not shown). The coated films were denser compared to that on the nickel network and their color was light gray.

3.2. Photocatalytic degradation by the non-calcinated TiO₂ film

3.2.1. Photocatalytic activity

In order to verify the photocatalytic activity of the non-calcinated TiO₂ film, two experiments were conducted at pH 7.0 and pH 2 (maximal photocatalytic activity, see Section 3.2.2) simultaneously, one with bare nickel network and the other with TiO₂ coated nickel network (four pieces). The initial MO concentrations

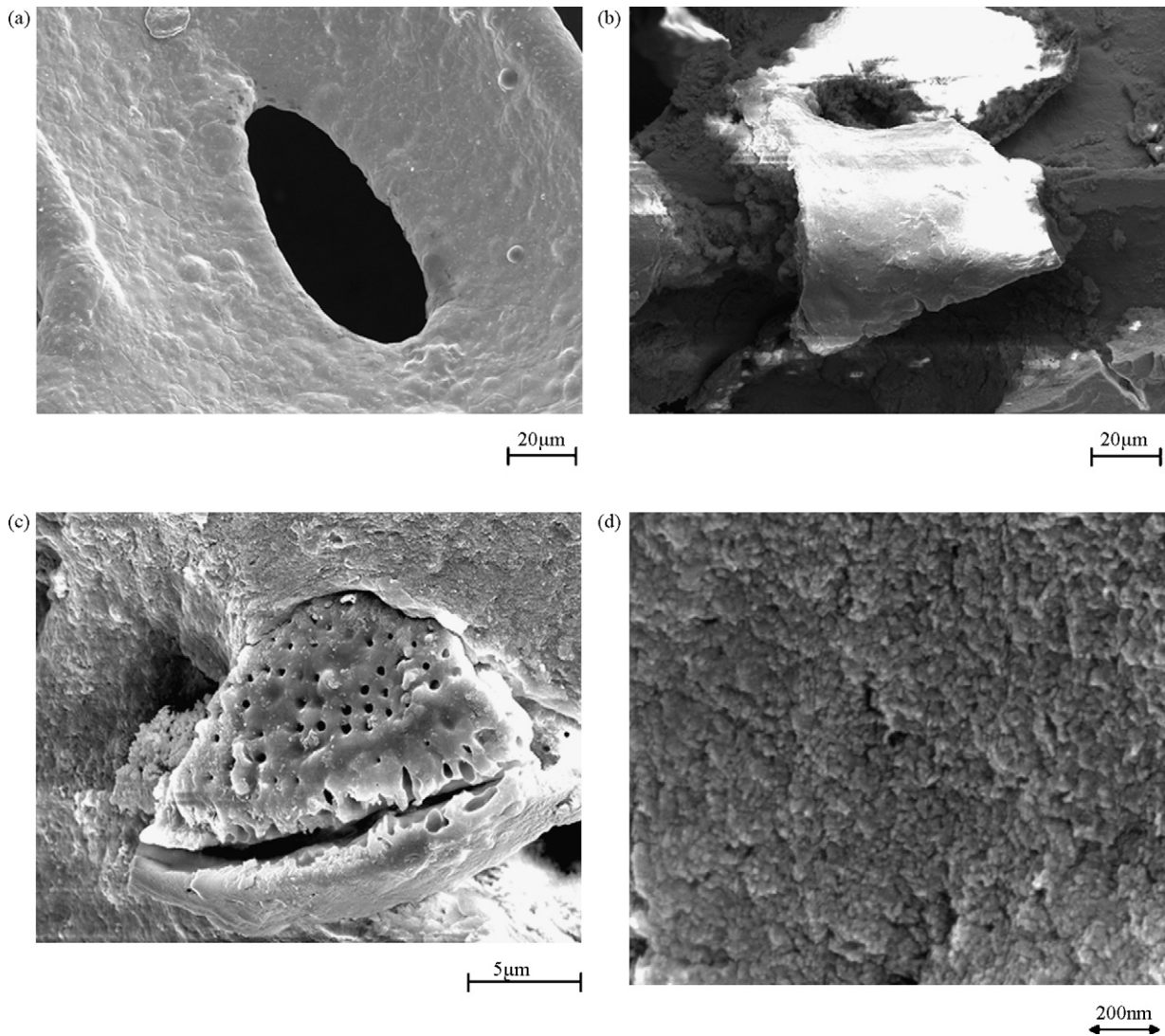


Fig. 2. FESEM images of Ni substrate (a) and TiO₂ particles coated on Ni substrate by electrophoretic deposition with 800× magnification (b), 5000× magnification (c) and 8000× magnification (d).

were 5 mg/L in both experiments. Fig. 4 shows the photocatalytic results (pH 7) after UV lamp illumination for 2 h. It was found that the degradation rate of MO with bare nickel network was $36.5 \pm 0.5\%$ ($n=3$) at pH 7 and $51.4 \pm 1.1\%$ ($n=3$) at pH 2, and the non-calculated TiO₂ film coated nickel network exhibited a much higher degradation rate of $75.2 \pm 1.7\%$ ($n=3$) at pH 7 and $95.5 \pm 1.5\%$ ($n=3$) at pH 2.

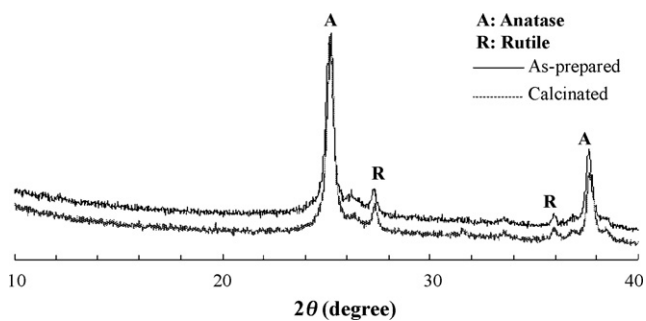


Fig. 3. X-ray patterns for the titania samples prepared by electrophoretic deposition, as-prepared and post-heated at 450 °C for 1 h (calcinated).

The non-calculated TiO₂ film had the same photocatalytic activity with the TiO₂ film calcinated at 450 °C for 1 h: the former showed a net degradation rate of 38.7% to MO at pH 7, and the latter degraded about 40.0% MO under the same condition.

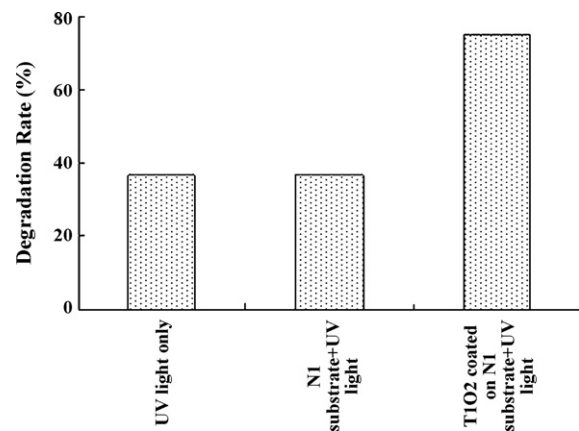


Fig. 4. Comparison of photocatalytic experiments: MO treated by UV only, by UV irradiated Ni substrate and by UV irradiated Ni substrate coated with the as-prepared TiO₂ film.

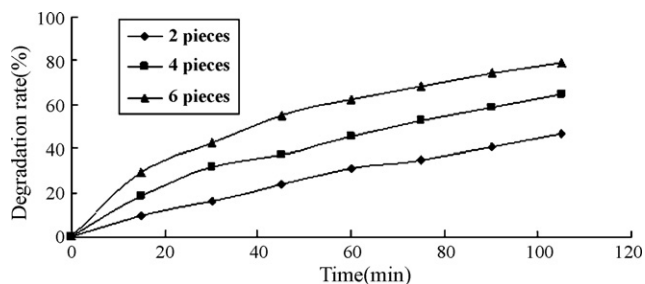


Fig. 5. Dependence of degradation rate of MO on the amount of the as-prepared TiO₂ coated on Ni substrate.

The degradation rate of MO with different amounts of TiO₂ was investigated and the results are shown in Fig. 5. The net degradation rates were $22.0 \pm 0.8\%$ ($n=3$) for two pieces of the non-calcinated TiO₂ film coated nickel network, $38.7 \pm 1.7\%$ ($n=3$) for four pieces and $48.7 \pm 1.7\%$ ($n=3$) for six pieces. The increased degradation rate with the amount of catalyst (TiO₂) further confirmed the photocatalytic activity of the novel non-calcinated TiO₂ film.

3.2.2. pH effect

Four pieces of the non-calcinated TiO₂ film coated nickel network were put into the reactor and the pH of the MO aqueous solution was adjusted by phosphate buffer. The relationship between degradation rate and pH is shown in Fig. 6. The degradation rate was $95.5 \pm 1.5\%$ ($n=3$) at pH 2.0, $75.2 \pm 1.7\%$ ($n=3$) at pH 7.0, and $83.3 \pm 1.8\%$ ($n=3$) at pH 10.0.

To clarify the effect of pH on the degradation rate of MO, we measured zeta potentials of catalysts at different pH values. When pH was lower than 7, the catalyst had positively charged surface, and higher pH (>7) made the surface negatively charged. This is in good agreement with the previous observation [26]. The lower pH produces more H⁺ that could adsorb on the surface of TiO₂, making TiO₂ particles positively charged. Positively charged TiO₂ particles assist the migration of photo-induced electrons, which could react with adsorbed O₂ to produce $\cdot\text{O}_2^-$ ($e^- + \text{O}_2 \rightarrow \cdot\text{O}_2^-$). In addition, positively charged TiO₂ particles could also inhibit the recombination of electrons and holes, generating more OH \cdot through the reaction between holes and water. Both radical ions $\cdot\text{O}_2^-$ and OH \cdot are strong oxidants [27,28] and could be responsible for the enhanced degradation of MO. Similarly, negatively charged in alkaline solutions is favorable for the migration of the hole to TiO₂ surface and generation of OH \cdot [29,30]. At neutral pH, the surface of TiO₂ is not charged, neither $\cdot\text{O}_2^-$ nor OH \cdot can be produced from the above pathways.

Acidic solutions were more effective in degrading MO than basic solutions. One possible reason is that sodium ions (dissociated from MO or buffer components) could react with adsorbed OH⁻ to generate -ONa, which reduced the amount of OH \cdot [31]. The other explanation could be pH increase that change MO from quinoid structure to azo structure [29], and quinoid structure is easier to degrade than azo structure. The validity of the latter was proved by

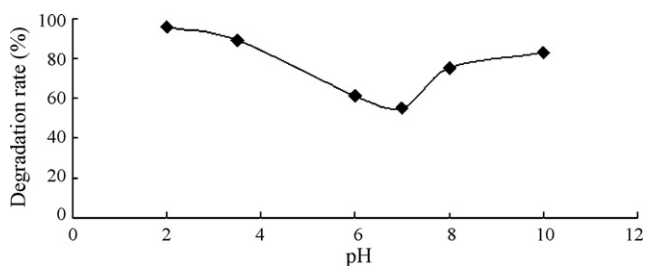


Fig. 6. Dependence of degradation rate of MO on pH. MO was degraded by four pieces of the as-prepared TiO₂ films irradiated by UV lamp.

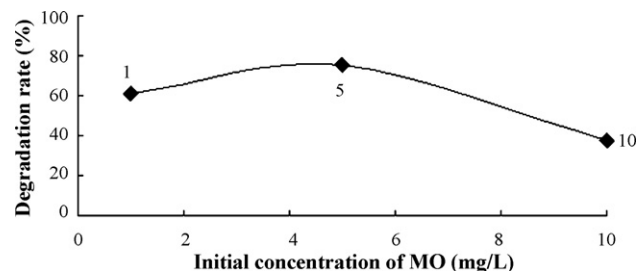


Fig. 7. Effects of MO solution initial concentrations on its photocatalytic degradation rate. Four pieces of the as-prepared TiO₂ films were used for the photocatalytic degradation of MO.

that the degradation rate of MO by UV lamp only increased from 36.5% to 51.4% with decreasing pH from 7 to 2.

3.2.3. The effects of MO initial concentration

The MO degradation by TiO₂ films was also investigated by changing the initial concentration of MO and the results are shown in Fig. 7. The degradation rate was $61.0 \pm 1.2\%$ ($n=3$) when MO initial concentration was 1 mg/L. It increased to $75.2 \pm 1.7\%$ ($n=3$) with 5 mg/L MO but decreased to $37.9 \pm 0.9\%$ ($n=3$) with 10 mg/L MO.

The degradation rate of MO was low at both higher and lower concentrations. Because the benzene ring on MO can absorb UV light at wavelength around 300 nm, when MO concentration is increased, the proportion of UV light absorbed by TiO₂ particles will decrease and result in the drop of the degradation rate. On the other hand, the chances of reaction of MO with electrons, holes and OH \cdot are less with the decrease in MO concentration, therefore the degradation of MO in a low concentration could not be effective by using photocatalyst. The phenomenon was also found in the photocatalytic treatment of other pollutants [32]. Too high pollutant concentration can cost more time and catalyst, and also produces lower degradation rate. However, if the pollutant concentration is very low, it is also difficult to be completely removed.

3.2.4. Kinetics analysis

The kinetic of photocatalytic degradation of MO solution was investigated when MO initial concentrations are 1 mg/L, 5 mg/L and 10 mg/L, respectively. The linear relationship between $\ln(C_0/C)$ and time (see Fig. 8) demonstrated that the photocatalytic degradation of MO followed a pseudo-first-order kinetics:

$$\ln \frac{C_0}{C} = kt \quad (3)$$

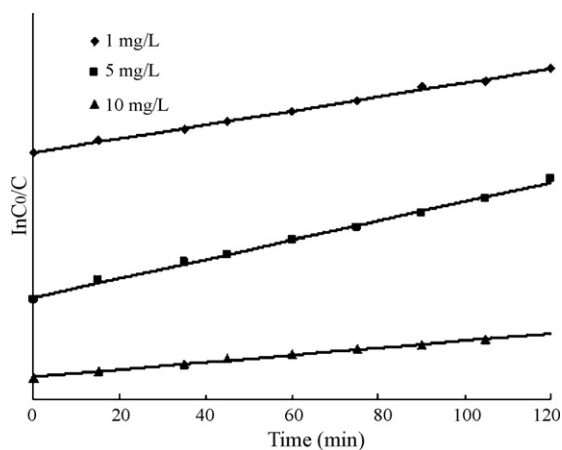


Fig. 8. $\ln(C_0/C)$ -time curves with different MO initial concentrations. Four pieces of the as-prepared TiO₂ films were used for the photocatalytic degradation of MO.

where C_0/C is the normalized MO concentration, t is the reaction time, and k is the reaction rate constant (min^{-1}). When MO initial concentration was 5 mg/L, the degradation rate was the highest among the three investigated concentrations, and the rate constant was calculated to be 0.0098 min^{-1} .

4. Conclusions

TiO₂ films were successfully prepared by a novel approach of electrophoretic deposition method without successive heat treatment. The non-calcinated TiO₂ films coated on nickel network exhibited a high photocatalytic activity to the degradation of MO. The photocatalytic degradation rate was improved with the increasing amount of TiO₂. Acidic solutions produced highest degradation rate and neutral pH was demonstrated to be least effective. The photocatalytic degradation of MO can be described with pseudo-first order reaction kinetics.

Acknowledgements

This work was supported by the Scientific Research Foundation for the Returned Overseas Chinese Scholars, State Education Ministry, the key project of Natural Science Foundation of Hubei Province (No. 2008CDA041) and the National Science Foundation of Huazhong University of Science and Technology.

References

- [1] A. Fujishima, K. Honda, Electrochemical photolysis of water at a semiconductor electrode, *Nature* 238 (1972) 37–38.
- [2] J.H. Carey, J. Lawrence, H.M. Tosine, Photodechlorination of PCBs in the presence of TiO₂ in aqueous suspensions, *Bull. Environ. Contam. Toxicol.* 16 (1976) 697–702.
- [3] H. Lin, X. Ji, Q. Chen, Y. Zhou, C.E. Craig, K. Wu, Mesoporous-TiO₂ nanoparticles based carbon paste electrodes exhibit enhanced electrochemical sensitivity for phenol, *Electrochem. Commun.* 11 (2009) 1990–1995.
- [4] J. Senthilnathan, L. Philip, Removal of mixed pesticides from drinking water system by photodegradation using suspended and immobilized TiO₂, *J. Environ. Sci. Health. B* 44 (2009) 262–270.
- [5] D.V. Sojic, V.B. Anderluh, D.Z. Orcic, B.F. Abramovic, Photodegradation of clopyralid in TiO₂ suspensions: identification of intermediates and reaction pathways, *J. Hazard. Mater.* 168 (2009) 94–101.
- [6] G. Perchet, G. Merlina, J.-C. Revel, M. Hafidi, C. Richard, E. Pinelli, Evaluation of TiO₂ photocatalysis treatment on nitrophenols and nitramines contaminated plant wastewaters by solid-phase extraction coupled with ESI HPLC–MS, *J. Hazard. Mater.* 166 (2009) 284–290.
- [7] Z. Yigit, H. Inan, A study of the photocatalytic oxidation of humic acid on anatase and mix-phase anatase–rutile TiO₂ nanoparticles, *Water Air Soil Pollut.* 9 (2009) 243–273.
- [8] X. Wang, Y. Liu, Zh. Hu, Y. Chen, W. Liu, G. Zhao, Degradation of methyl orange by composite photocatalysis nano-TiO₂ immobilized on activated carbons of different porosities, *J. Hazard. Mater.* 169 (2009) 1061–1067.
- [9] M. Antoniadou, P. Lianos, Photoelectrochemical oxidation of organic substances over nanocrystalline titania: optimization of the photoelectrochemical cell, *Catal. Today* 144 (2009) 166–171.
- [10] F. Han, V.S.R. Kambala, M. Srinivasan, D. Rajarathnam, R. Naidu, Tailored titanium dioxide photocatalysts for the degradation of organic dyes in wastewater treatment: a review, *Appl. Catal. A-Gen.* 359 (2009) 25–40.
- [11] M. Faramarzpour, M. Vossoughi, M. Borghei, Photocatalytic degradation of furfural by titania nanoparticles in a floating-bed photoreactor, *Chem. Eng. J. (Amsterdam, Netherlands)* 146 (2009) 79–85.
- [12] E. Szabo-Bardos, Z. Zsilak, O. Horvath, Photocatalytic degradation of anionic surfactant in titanium dioxide suspension, *Prog. Colloid Polym. Sci.* 135 (2008) 21–28.
- [13] K. Esquivel, L.G. Arriaga, F.J. Rodriguez, L. Martinez, L.A. Godinez, Development of a TiO₂ modified optical fiber electrode and its incorporation into a photoelectrochemical reactor for wastewater treatment, *Water Res.* 43 (2009) 3593–3603.
- [14] H. Choi, S.R. Al-Abed, D.D. Dionysiou, Nanostructured titanium oxide film and membrane-based photocatalysis for water treatment, in: M. DiAllo, J. Duncan, N. Savage, A. Street, R. Sustich (Eds.), *Nanotechnology Applications for Clean Water*, William Andrew Inc., Norwich, NY, 2009, pp. 39–46.
- [15] X. Chen, S.S. Mao, Titanium dioxide nanomaterials: synthesis, properties, modifications, and applications, *Chem. Rev.* 107 (2007) 2891–2959.
- [16] Y. Lei, L.D. Zhang, J.C. Fan, Fabrication, characterization and Raman study of TiO₂ nanowire arrays prepared by anodic oxidative hydrolysis of TiCl₃, *Chem. Phys. Lett.* 338 (2001) 231–236.
- [17] S. Liu, K. Huang, Straightforward fabrication of highly ordered TiO₂ nanowire arrays in AAM on aluminum substrate, *Sol. Energ. Mater. Sol. C* 85 (2004) 125–131.
- [18] K. Shankar, J.I. Basham, N.K. Allam, O.K. Varghese, G.K. Mor, X. Feng, M. Paulose, J.A. Seabold, K.-Sh. Choi, C.A. Grimes, Recent advances in the use of TiO₂ nanotube and nanowire arrays for oxidative photoelectrochemistry, *J. Phys. Chem. C* 113 (2009) 6327–6359.
- [19] Ch. Bac, Y. Yoon, H. Yoo, D. Han, J. Cho, B.H. Lee, M.M. Sung, M. Lee, J. Kim, H. Shin, Controlled fabrication of multiwall anatase TiO₂ nanotubular architectures, *Chem. Mater.* 21 (2009) 2574–2576.
- [20] G. Zhang, H. Huang, Y. Liu, L. Zhou, Fabrication of crack-free anodic nanoporous titania and its enhanced photoelectrochemical response, *Appl. Catal. B-Environ.* 90 (2009) 262–267.
- [21] J.M. Peralta-Hernandez, J. Manriquez, Y. Meas-Vong, F.J. Rodriguez, Th.W. Chapman, M.I. Maldonado, L.A. Godinez, Photocatalytic properties of nanostructured TiO₂-carbon films obtained by means of electrophoretic deposition, *J. Hazard. Mater.* 147 (2007) 588–593.
- [22] M. Zhou, J. Yu, Sh. Liu, P. Zhai, L. Jiang, Effects of calcination temperatures on photocatalytic activity of SnO₂/TiO₂ composite films prepared by an EPD method, *J. Hazard. Mater.* 154 (2008) 1141–1148.
- [23] T. Kurosaki, A. Nakagawa, Sh. Iimura, S. Yoshihara, T. Shirakashi, Photocatalytic properties of titanium oxide film prepared by electrophoretic sol–gel deposition, *Electrochemistry (Tokyo, Japan)* 70 (2002) 860–862.
- [24] W.-Ch. Hung, Y.-Ch. Chen, H. Chu, T.-K. Tseng, Synthesis and characterization of TiO₂ and Fe/TiO₂ nanoparticles and the performance for photocatalytic degradation of 1,2-dichloroethane, *Appl. Surf. Sci.* 255 (2008) 2205–2213.
- [25] Ch. Kim, J.-T. Kim, K.-S. Kim, S. Jeong, H.-Y. Kim, Y.-S. Han, Immobilization of TiO₂ on an ITO substrate to facilitate the photoelectrochemical degradation of an organic dye pollutant, *Electrochim. Acta* 54 (2009) 5715–5720.
- [26] K. Watanabe, D. Tipayarom, L. Laokiat, N. Grisdanurak, Sonophotocatalytic activity of methyl orange over Fe(III)/TiO₂, *React. Kinet. Catal. Lett.* 97 (2009) 249–254.
- [27] D. Wang, J. Zhang, Q. Luo, X. Li, Y. Duan, J. An, Characterization and photocatalytic activity of poly(3-hexylthiophene)-modified TiO₂ for degradation of methyl orange under visible light, *J. Hazard. Mater.* 169 (2009) 546–550.
- [28] P. Salvador, On the nature of photogenerated radical species active in the oxidative degradation of dissolved pollutants with TiO₂ aqueous suspensions: a revision in the light of the electronic structure of adsorbed water, *J. Phys. Chem. C* 111 (2007) 17038–17043.
- [29] N. Barka, A. Assabbane, A. Nounah, J. Dussaud, Y.A. Ichou, Photocatalytic degradation of methyl orange with immobilized TiO₂ nanoparticles: effect of pH and some inorganic anions, *Phys. Chem. News* 41 (2008) 85–88.
- [30] L. Gan, X. Wang, Zh. Hao, Photocatalytic degradation of methylene blue with TiO₂/SiO₂ aerogels, *Tongji Daxue Xuebao Ziran Kexunban* 33 (2005) 1078–1082.
- [31] J. Wang, B. Xin, H. Yu, Research on photocatalytic degradation of rhodamine B with Fe³⁺ doped TiO₂/SiO₂ system, *Gaodeng Xuexiao Huaxue Xuebao* 24 (2003) 1093–1096.
- [32] N.F. Zainudin, A.Z. Abdullah, A.R. Mohamed, Characteristics of supported nano-TiO₂/ZSM-5/silica gel (SNTZS): photocatalytic degradation of phenol, *J. Hazard. Mater.* 174 (2010) 299–306.